

Crossed Topology in Two-Loop Dispersive Approach

A. Aleksejevs

Grenfell Campus of Memorial University, Canada

We extend existing dispersive approach in subloop insertion to the case of crossed two-loop box type topologies. Based on the ideas of the Feynman trick, mass shift approach and dispersive representation of two-point Passarino-Veltman function we expressed two-loop scalar diagrams in the compact analytical form suitable for the automatization of the calculations. The results are expressed in a way that the numerical integration over Feynman and dispersive parameters and differentiation with respect to mass shift parameters are required in the final stage only.

I. INTRODUCTION

The experimental searches for the physics beyond the standard model such as MOLLER [1] frequently require calculations of the observables to a high degree of precision. This can be achieved by accounting for the next-to-next to leading order (NNLO) perturbative contributions in the scattering matrix element. That translates to the evaluations of two-loop Feynman diagrams, but in general this is not a trivial task. Particularly, a full set of two-loop electroweak corrections is close to impossible task to complete without some sort of automatization, and tremendous effort is already invested in the development of the various approaches for evaluation of the two-loop diagrams. Development of the techniques in the two-loop self-energies and vertex functions calculations is outlined in [2–5] and has been extended in more recent work of [6–11]. Two-loop n -point integrals have been evaluated in [12, 13] using techniques of sector decomposition. In electroweak physics, authors in [14] studied two-loop fermionic contributions to the effective Weinberg mixing angle. Two-loop electroweak corrections to the $M_W - M_Z$ mass correlation was studied in [15]. In [16–19], the effort was directed to the studies of dominant contributions of the two-loop electroweak corrections to the parity-violating asymmetry in Moller scattering. In [20], a general approach was developed to deal with the two-loop diagrams calculations in the case of arbitrary tensor structure, which employed an idea of dispersive subloop insertion. A general notion outlined in [20] is that for many two-loop topologies it is possible to join all but one

propagators in the sub-loop insertion in a way that integration momenta of the second loop is not present when applying Feynman trick. This way, it was possible to reduce subloop insertion to two-point Passarino-Veltman function and later replace subloop insertion by the effective propagator using dispersive representation. After that, the second loop integration can be carried out analytically in the Passarino-Veltman basis. In this paper, we extend our approach used in [20] to the cases where subloop insertion has crossed-box type of topology. For this topology, it is not possible to join all propagators except one, as we did before, and hence it would be problematic to reduce subloop insertion to two-point function using the same approach. Solution to this problem can be found in the application of the Feynman trick to the groups of the propagators each carrying the same integration momenta of the both loops. Thus, we can reduce crossed subloop insertion to two-point function. In this paper, we start with the general outline of the methods proposed in [20] and then consider two specific two-loop topologies, crossed two-loop vertex and box diagrams, and develop a generalized approach on how to treat crossed subloop insertion in two-loop calculations.

II. SUBLOOP INSERTION

Idea of the subloop insertion was employed in [20] for the case of two-loop topologies. Before considering crossed two-loop triangle and box topology, let us review general ideas developed in [20] for the triangle and box type subloop insertion. Let us start with two-loop triangle topology shown on Fig.(1). To simplify our derivations, we consider the case where all the couplings are set to one, and all the particles are scalars. We will assume that particles carrying momenta k_1 and k_2 are on-shell, and particle with momentum k_3 is off-shell. Here, we can write

$$I_{\Delta_1} = -\frac{1}{\pi^4} \int \frac{d^4 q_1 d^4 q_2}{[(k_1 - q_1)^2 - m_1^2][(k_2 - q_1)^2 - m_1^2][(q_1 - q_2)^2 - m_a^2][(k_2 - q_2)^2 - m_1^2]} \times \frac{1}{[q_2^2 - m_b^2][(k_1 - q_2)^2 - m_1^2]}. \quad (1)$$

The first three propagators in Eq.(1) belong to the triangle insertion (red and bold) in Fig.(1). Initial step is to join first two propagators, without momenta of the second loop,

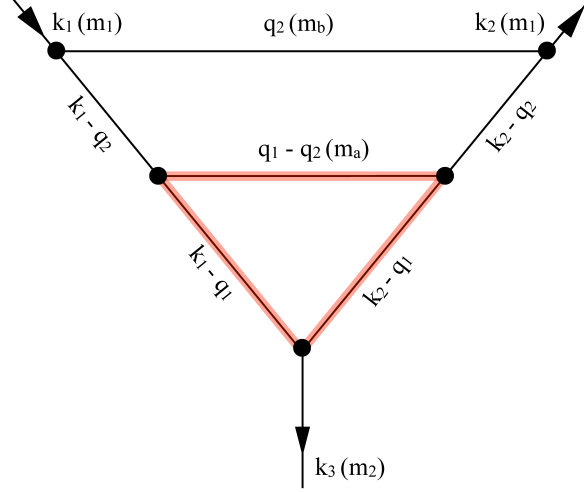


Figure 1: Two-loop triangle topology with triangle type insertion. Red and bold selection corresponds to the triangle subloop insertion.

using Feynman trick:

$$I_{\Delta_1} = -\frac{1}{\pi^4} \int_0^1 dx \int \frac{d^4 q_1 d^4 q_2}{[(q_1 - (xk_1 + \bar{x}k_2))^2 - (xk_1 + \bar{x}k_2)^2]^2 [(q_1 - q_2)^2 - m_a^2] [(k_2 - q_2)^2 - m_1^2]} \times \frac{1}{[q_2^2 - m_b^2] [(k_1 - q_2)^2 - m_1^2]}, \quad (2)$$

where $\bar{x} = 1 - x$. Quadratic form in Eq.(2) can be removed if we apply so-called mass shift approach:

$$\frac{1}{[(q_1 - (xk_1 + \bar{x}k_2))^2 - (xk_1 + \bar{x}k_2)^2]^2} = \lim_{\lambda \rightarrow 0} \frac{\partial}{\partial \lambda} \frac{1}{(q_1 - (xk_1 + \bar{x}k_2))^2 - ((xk_1 + \bar{x}k_2)^2 + \lambda)}. \quad (3)$$

After substituting momentum $q_1 = \tau + xk_1 + \bar{x}k_2$ and using Eq.(3), we can replace the first loop integral in Eq.(2) by two-point Passarino-Veltman function:

$$I_{\Delta_1} = -\frac{i}{\pi^2} \lim_{\lambda \rightarrow 0} \frac{\partial}{\partial \lambda} \int_0^1 dx \int d^4 q_2 \frac{B_0[(q_2 - xk_1 - \bar{x}k_2)^2, m_\lambda^2, m_a^2]}{[(k_2 - q_2)^2 - m_1^2] [q_2^2 - m_b^2] [(k_1 - q_2)^2 - m_1^2]}. \quad (4)$$

Here, $m_\lambda^2 = (xk_1 + \bar{x}k_2)^2 + \lambda = m_1^2 - x\bar{x}k_3^2 + \lambda$. The next step is to apply dispersive replacement of the two-point function:

$$I_{\Delta_1} = \frac{i}{\pi^3} \lim_{\lambda \rightarrow 0} \frac{\partial}{\partial \lambda} \int_0^1 dx \int_{(m_a+m_\lambda)^2}^{\Lambda^2} ds \Im B_0 [s, m_\lambda^2, m_a^2] \\ \times \int \frac{d^4 q_2}{[(k_2 - q_2)^2 - m_1^2] [q_2^2 - m_b^2] [(k_1 - q_2)^2 - m_1^2] [(q_2 - xk_1 - \bar{x}k_2)^2 - s - i\epsilon]}. \quad (5)$$

As a result, the denominator $\frac{1}{(q_2 - xk_1 - \bar{x}k_2)^2 - s - i\epsilon}$, which is coming from dispersive representation of two-point function in Eq.(4), is absorbed into the second loop integration as an additional propagator. As it was discussed in [20], effective mass parameter m_λ^2 could become negative (if $k_3^2 > \frac{m_1^2 + \lambda}{x\bar{x}}$) and that requires a different treatment of dispersive integral. This is discussed in details in [1] and it is straightforward to implement the case where $m_\lambda^2 < 0$. To avoid lengthy expressions, we will assume a condition where m_λ^2 is positive. In the next step, in Eq.(5), we can apply Feynman trick to the first three propagators, and after using mass shift approach we can write the final two-loop result in two-point function basis:

$$I_{\Delta_1} = -\frac{1}{\pi} \lim_{\{\lambda, \delta\} \rightarrow 0} \frac{\partial^3}{\partial \lambda \partial \delta^2} \int_0^1 dx dy \int_0^{1-y} dz \int_{(m_a+m_\lambda)^2}^{\Lambda^2} ds \Im B_0 [s, m_\lambda^2, m_a^2] \\ \times B_0 [((y - \bar{x})k_2 + (z - x)k_1)^2, m_\delta^2, s]. \quad (6)$$

Effective mass m_δ^2 is defined as follows: $m_\delta^2 = (\bar{y} - z)m_b^2 + (y + z)m_1^2 - yzk_3^2 + \delta$. Integration cutoff Λ^2 is introduced in order to keep the integration finite. After differentiation with respect to λ and δ , the dependence on cutoff and regularization parameters in Eq.(6) will cancel. Using the approach outlined in derivation of Eq.(6), we can express two-loop triangle graph with arbitrary tensorial rank in two-point function basis analytically, and later perform integration and differentiation numerically. If there are ultraviolet divergences, they can be addressed by employing the subloop subtraction in a given renormalization scheme. In this case, the dispersive integral in Eq.(6) will have a singly- or doubly-subtracted structure. The second loop renormalization can be achieved by adding second-order counter terms, also computed using dispersive representation. The same ideas can be applied to the box

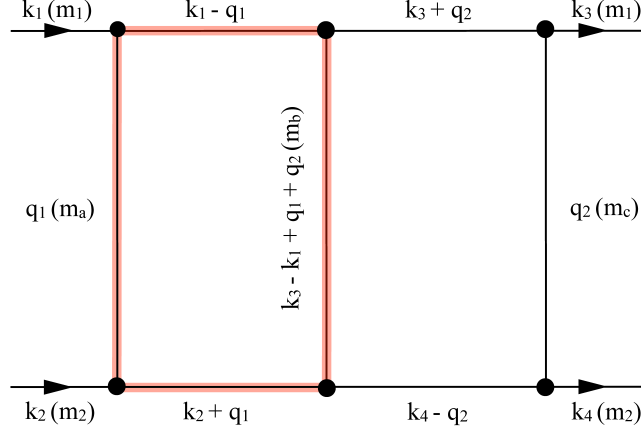


Figure 2: Two-loop box topology (double box) with box type insertion. Red and bold selection corresponds to the box subloop insertion.

subloop. If we consider the diagram on Fig.(2), we can write the following:

$$I_{\square_1} = -\frac{1}{\pi^4} \int \frac{d^4 q_1 d^4 q_2}{[q_1^2 - m_a^2] [(k_1 - q_1)^2 - m_1^2] [(k_2 + q_1)^2 - m_2^2] [(k_3 - k_1 + q_1 + q_2)^2 - m_b^2]} \times \frac{1}{[q_2^2 - m_c^2] [(k_4 - q_2)^2 - m_2^2] [(k_3 + q_2)^2 - m_1^2]}. \quad (7)$$

After joining the first three propagators, shifting momentum $q_1 = \tau - q_2 - k_3 + k_1$, and expressing two-point function by dispersive integral, we can write:

$$I_{\square_1} = \frac{i}{\pi^3} \lim_{\lambda \rightarrow 0} \frac{\partial^2}{\partial \lambda^2} \int_0^1 dx \int_0^{1-x} dy \int_{(m_b+m_\lambda)^2}^{\Lambda^2} ds \Im B_0 [s, m_b^2, m_\lambda^2] \times \int \frac{d^4 q_2}{[q_2^2 - m_c^2] [(k_4 - q_2)^2 - m_2^2] [(k_3 + q_2)^2 - m_1^2] [(q_2 + k_3 - x k_2 - k_1 \bar{y})^2 - s - i\epsilon]}. \quad (8)$$

Here, effective mass m_λ defined as $m_\lambda^2 = m_a^2 (\bar{x} - y) + x^2 m_2^2 + y^2 m_1^2 - 2xy (k_1 k_2) + \lambda$. In the same way as before, after joining the first three propagators in the second loop integral, we

get the following two-loop box result:

$$\begin{aligned}
I_{\square_1} = & -\frac{1}{\pi} \lim_{\lambda \rightarrow 0} \frac{\partial^4}{\partial \lambda^2 \partial \delta^2} \int_0^1 dx dz \int_0^{1-x} dy \int_0^{1-z} d\omega \int_{(m_b+m_\lambda)^2}^{\Lambda^2} ds \Im B_0 [s, m_b^2, m_\lambda^2] \\
& \times B_0 [(\omega k_4 + \bar{z} k_3 - x k_2 - \bar{y} k_1)^2, m_\delta^2, s].
\end{aligned} \tag{9}$$

Effective mass m_δ has the following structure: $m_\delta^2 = m_c^2 (\bar{z} - \omega) + m_1^2 z^2 + m_2^2 \omega^2 - 2z\omega (k_3 k_4) + \delta$. Results in both Eq.(6) and (9) are in compact form and can be implemented in computer algebra-based packages. Endpoint for two-loop calculations would be numerical evaluation of derivatives with respect to mass shift parameters, Feynman and dispersion integrals. Both examples which we have considered here assume that it is possible to join all propagator except one in the subloop insertion. All joined propagators should carry integration momentum of the subloop insertion only. As a result, subloop integral can be replaced by the two-point function. However, in the case of crossed two-loop topologies, it is not possible to achieve the same using the outlined approach directly. Crossed two-loop topologies will have box type insertion subloop with more than one propagator carrying integration momenta of the first and second loop. In the next section, we will consider two examples of crossed two-loop topology, from which we develop an approach allowing us to express subloop insertion in the two-point function basis, allowing to write final expressions in a compact form suitable for the numerical evaluations.

III. CROSSED TOPOLOGY SUBLOOP INSERTION

A. Two-Loop Crossed Triangle

Let us start with the two-loop topology shown on Fig.(3). Particles with momenta q_1 , q_2 and k_3 have masses m_a , m_b and m_3 , respectively. All other lines on graph from Fig.(3) have the mass m_1 . We will employ the same idea of dispersive insertion as before, with the final two-loop result will be given completely in two-point Passarino-Veltman function basis. According to the momenta distribution on Fig.(3), we can write the following:

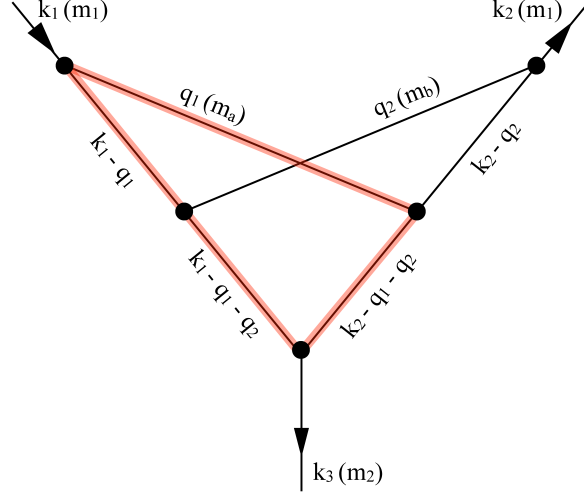


Figure 3: Crossed two-loop vertex topology.

$$I_{\Delta_2} = -\frac{1}{\pi^4} \int \frac{d^4 q_1 d^4 q_2}{[q_1^2 - m_a^2] [(k_1 - q_1)^2 - m_1^2] [(k_1 - q_1 - q_2)^2 - m_1^2] [(k_2 - q_1 - q_2)^2 - m_1^2]} \times \frac{1}{[q_2^2 - m_b^2] [(k_2 - q_2)^2 - m_1^2]}. \quad (10)$$

As noted before, the subloop insertion in Fig.(3) has only two propagators without the momentum of the second loop. In order to reduce subloop into two-point function, we will join the first and second propagators and then third and fourth. In this case we get the following:

$$I_{\Delta_2} = -\frac{1}{\pi^4} \lim_{\{\xi, \lambda\} \rightarrow 0} \frac{\partial^2}{\partial \xi \partial \lambda} \int_0^1 dx dy \int \frac{d^4 q_2}{[q_2^2 - m_b^2] [(k_2 - q_2)^2 - m_1^2]} \times \int \frac{d^4 q_1}{[(q_1 - k_1 x)^2 - m_\xi^2] [(q_1 + q_2 - \bar{y} k_2 - y k_1)^2 - m_\lambda^2]}. \quad (11)$$

Here, masses m_ξ^2 and m_λ^2 are defined as $m_\xi^2 = m_a^2 \bar{x} + m_1^2 x^2 + \xi$ and $m_\lambda^2 = m_1^2 - \bar{y} y k_3^2 + \lambda$. Thus, the loop integral over q_1 , after replacing $q_1 = \tau + k_1 x$, now can be written as a two-point function:

$$I_{\Delta_2} = -\frac{i}{\pi^2} \lim_{\{\xi, \lambda\} \rightarrow 0} \frac{\partial^2}{\partial \xi \partial \lambda} \int_0^1 dx dy \int d^4 q_2 \frac{B_0 [(q_2 - \bar{y} k_2 + k_1 (x - y))^2, m_\xi^2, m_\lambda^2]}{[q_2^2 - m_b^2] [(k_2 - q_2)^2 - m_1^2]}. \quad (12)$$

After replacing the two-point function by it's dispersive representation, we can address evaluation of the second loop integral:

$$I_{\Delta_2} = \frac{i}{\pi^3} \lim_{\{\xi, \lambda\} \rightarrow 0} \frac{\partial^2}{\partial \xi \partial \lambda} \int_0^1 dx dy \int_{(m_\xi + m_\lambda)^2}^{\Lambda^2} ds \Im B_0 [s, m_\xi^2, m_\lambda^2] \\ \times \int \frac{d^4 q_2}{[q_2^2 - m_b^2] [(k_2 - q_2)^2 - m_1^2] [(q_2 - \bar{y} k_2 + k_1 (x - y))^2 - s - i\epsilon]}. \quad (13)$$

Now, after joining the first two propagators in Eq.(13) and introducing mass shift parameter ϕ , the final result for the graph on Fig.(3) can be expressed in terms of the product of two two-point functions, which are later integrated and then numerically differentiated:

$$I_{\Delta_2} = -\frac{1}{\pi} \lim_{\{\xi, \lambda, \phi\} \rightarrow 0} \frac{\partial^3}{\partial \xi \partial \lambda \partial \phi} \int_0^1 dx dy dz \int_{(m_\xi + m_\lambda)^2}^{\Lambda^2} ds \Im B_0 [s, m_\xi^2, m_\lambda^2] \\ \times B_0 [((z - \bar{y}) k_2 + k_1 (x - y))^2, m_\phi^2, s]. \quad (14)$$

Here, mass m_ϕ^2 has the following structure: $m_\phi^2 = m_b^2 \bar{z} + m_1^2 z^2 + \phi$. Eqs.(6) and (14) have the same dimension of multidimensional integration and the same overall order of the differentiation with respect to the mass shift parameters. In addition to that, in the derivation of Eq.(14), we had to introduce one extra mass shift parameter. It is obvious that in the crossed-type subloop insertion we would have to deal with four propagators. General structure of the insertion would have two groups of propagators with the similar momenta in each group. That allows us to join propagators in two groups separately and effectively reduce an entire insertion to the two-point function. The same approach could be implemented for the two-loop crossed box topology discussed in the next subsection.

B. Two-Loop Crossed Box

Let us start by writing a general expression for the two-loop integral for a crossed two-loop box topology shown on Fig.(4):

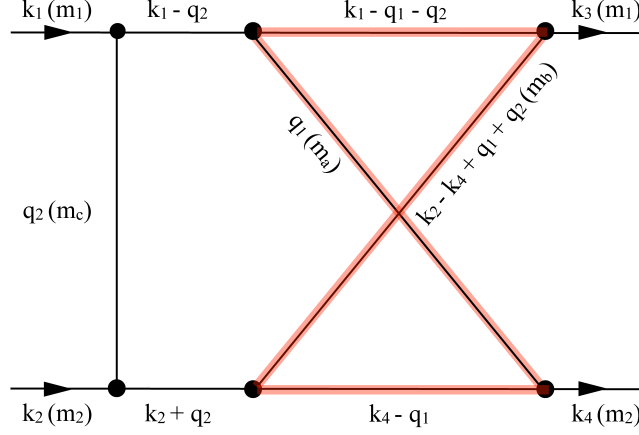


Figure 4: Crossed two-loop box topology.

$$I_{\square_2} = -\frac{1}{\pi^4} \int \frac{d^4 q_1 d^4 q_2}{[q_1^2 - m_a^2] [(k_4 - q_1)^2 - m_2^2] [(k_2 - k_4 + q_1 + q_2)^2 - m_b^2] [(k_1 - q_1 - q_2)^2 - m_1^2]} \times \frac{1}{[q_2^2 - m_c^2] [(k_1 - q_2)^2 - m_1^2] [(k_2 + q_2)^2 - m_2^2]}. \quad (15)$$

After joining the first and the second, and then the third and the fourth propagators, we can write, with the help of two mass shift parameters ξ and λ , the following:

$$I_{\square_2} = -\frac{i}{\pi^2} \lim_{\{\xi, \lambda\} \rightarrow 0} \frac{\partial^2}{\partial \xi \partial \lambda} \int_0^1 dx dy \int d^4 q_2 \frac{B_0 [(q_2 - xk_4 + yk_3 - k_1)^2, m_\xi^2, m_\lambda^2]}{[q_2^2 - m_c^2] [(k_1 - q_2)^2 - m_1^2] [(k_2 + q_2)^2 - m_2^2]}, \quad (16)$$

where $m_\xi^2 = \bar{x}m_a^2 + x^2m_2^2 + \xi$ and $m_\lambda^2 = \bar{y}^2m_1^2 + ym_b^2 + \lambda$. Replacing two-point function in Eq.(16) by a dispersion integral, we arrive to:

$$I_{\square_2} = \frac{i}{\pi^3} \lim_{\{\xi, \lambda\} \rightarrow 0} \frac{\partial^2}{\partial \xi \partial \lambda} \int_0^1 dx dy \int_{(m_\xi + m_\lambda)^2}^{\Lambda^2} ds \Im B_0 [s, m_\xi^2, m_\lambda^2] \times \int \frac{d^4 q_2}{[q_2^2 - m_c^2] [(k_1 - q_2)^2 - m_1^2] [(k_2 + q_2)^2 - m_2^2] [(q_2 - xk_4 + yk_3 - k_1)^2 - s - i\epsilon]}. \quad (17)$$

The second loop integration is done after joining first three propagators in the integral over q_2 and introducing third mass shift parameter δ :

$$I_{\square_2} = -\frac{1}{\pi} \lim_{\{\xi, \lambda\} \rightarrow 0} \frac{\partial^4}{\partial \xi \partial \lambda \partial \delta^2} \int_0^1 dx dy dz \int_0^{1-z} dw \int_{(m_\xi + m_\lambda)^2}^{\Lambda^2} ds \Im B_0 [s, m_\xi^2, m_\lambda^2] \\ \times B_0 [(\bar{z}k_1 + \omega k_2 + xk_4 - yk_3)^2, m_\delta^2, s], \quad (18)$$

where $m_\delta^2 = (\bar{z} - \omega) m_c^2 + (\omega k_2 - z k_1)^2 + \delta$. The crossed two-loop box also acquires an additional mass shift parameter, while a degree of multidimensional integration and general order of differentiation remains the same as in Eq.(9). It is evident that in both cases reflected on Fig.(3) and Fig.(4), we are dealing with the box-type insertion. In the cases without a crossed topology, external legs of an insertion would carry momentum of the second loop sequentially. For example, if we have external momenta labeled as p_1, p_2, p_3 and p_4 , the second loop momentum shows up in the combinations of momenta $\{p_1, p_2\}, \{p_2, p_3\}, \{p_3, p_4\}$ and $\{p_1, p_4\}$. This will allow us to join three propagators without momentum of the second loop, and arrive to the results for the box-type insertion outlined in [1]. The crossed-type box insertions will have the second loop momentum appear in the combinations of external momenta such as $\{p_1, p_3\}$ and $\{p_2, p_4\}$. As a result, we would have to apply Feynman trick to two groups of propagators. At this point, we will consider a general case of the crossed box type subloop insertion. For the crossed box subloop, shown on Fig.(5), we will assume that external momenta p_2 and p_4 would depend on the momentum of the second loop. In this case, we can write:

$$I_{\boxtimes} = \frac{1}{i\pi^2} \int \frac{d^4 q}{[q^2 - m_1^2] [(q + p_1)^2 - m_2^2] [(q + p_1 + p_2)^2 - m_3^2] [(q + p_1 + p_2 + p_3)^2 - m_4^2]}. \quad (19)$$

As it was considered in the previous examples, we will join propagators in Eq.(19) in two groups: the first and the second, and then the third and the fourth. After introducing two mass shift parameters, and shifting momentum of integration $q = \tau - xp_1$, we can rewrite Eq.(19) in the two-point function basis:

$$I_{\boxtimes} = \lim_{\{\xi, \lambda\} \rightarrow 0} \frac{\partial^2}{\partial \xi \partial \lambda} \int_0^1 dx dy B_0 [(\bar{x}p_1 + p_2 + yp_3)^2, m_\xi^2, m_\lambda^2]. \quad (20)$$

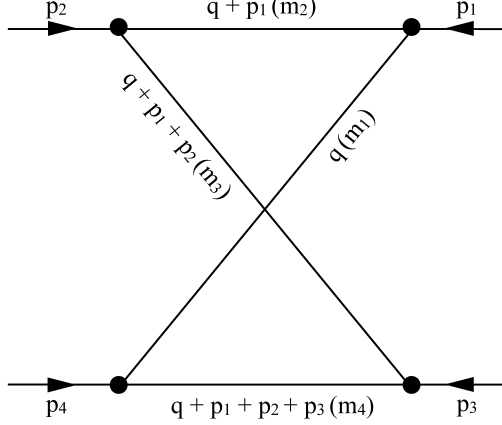


Figure 5: General crossed box subloop.

Here, $m_\xi^2 = \bar{x}m_1^2 + xm_2^2 - x\bar{x}p_1^2 + \xi$ and $m_\lambda^2 = \bar{y}m_3^2 + ym_4^2 + p_1^2 + yp_3^2 + \lambda$. Replacing the two-point function in Eq.(20) by a dispersive representation, we arrive to the following result:

$$I_{\boxtimes} = -\frac{1}{\pi} \lim_{\{\xi, \lambda\} \rightarrow 0} \frac{\partial^2}{\partial \xi \partial \lambda} \int_0^1 dx dy \int_{(m_\xi + m_\lambda)^2}^{\Lambda^2} ds \frac{\Im B_0 [s, m_\xi^2, m_\lambda^2]}{(\bar{x}p_1 + p_2 + yp_3)^2 - s - i\epsilon}. \quad (21)$$

The Eq.(21) suggests that in general, if we encounter crossed box subloop insertion, we can replace it by the effective four-particle coupling:

$$\Gamma_{\boxtimes} = \hat{\mathbf{D}} \left[\frac{\Im B_0 [s, m_\xi^2, m_\lambda^2]}{(\bar{x}p_1 + p_2 + yp_3)^2 - s - i\epsilon} \right], \quad (22)$$

with operator $\hat{\mathbf{D}}$ is defined as $\hat{\mathbf{D}} = \lim_{\{\xi, \lambda\} \rightarrow 0} \frac{\partial^2}{\partial \xi \partial \lambda} \int_0^1 dx dy \int_{(m_\xi + m_\lambda)^2}^{\Lambda^2} ds \dots$. Using Eq.(22), we can perform the second loop integration in the two-point function basis, and at the end evaluate derivatives and integrals numerically. In general, it is straightforward to extend this approach to the cases with tensor-type numerator which was considered in details in [20].

IV. CONCLUSION

In this work, we have addressed a specific type of the crossed topologies arising in the two-loop triangle and box graphs. Based on the examples outlined in the paper, we have developed an approach where crossed subloop insertion can be replaced by two-point function basis. Later, the two-point function can be represented by a dispersive integral and an

arising propagator-like term can be moved to the second loop integration. The second loop integration can also be reduced into the two-point function representation. As a result, we can express the two-loop matrix elements analytically in a rather compact form, and the scalar integration over Feynman parameter space and dispersive integration and differentiation with respect to mass-shift parameters can be carried out numerically at the last stage. This way, we can address the problem of the much-needed complete electroweak two-loop calculation by automatization of the entire process.

Acknowledgments

Author is grateful to S. Barkanova for stimulating and inspiring discussions. This work was supported by National Science and Engineering Research Council (NSERC) of Canada.

-
- [1] MOLLER Collaboration (J. Benesch et al.), JLAB-PHY-14-1986, arXiv:1411.4088, (2014).
 - [2] D. Kreimer, Phys. Lett. B 273, 277 (1991).
 - [3] S. Bauberger and M. Böhm, Nucl. Phys. B445, 25-46 (1995).
 - [4] A. Czarnecki, U. Kilian, and D. Kreimer, Nucl. Phys. B433, 259 (1995).
 - [5] A. Frink, U. Kilian, and D. Kreimer, Nucl. Phys. B488, 426 (1997).
 - [6] L. Adams, C. Bogner, and S. Weinzierl, J. Math. Phys. 54, 052303 (2013).
 - [7] L. Adams, C. Bogner, and S. Weinzierl, J. Math. Phys. 56, 072303 (2015).
 - [8] L. Adams, C. Bogner, and S. Weinzierl, J. Math. Phys. 57, 032304 (2016).
 - [9] E. Remiddi and L. Tancredi, Nucl. Phys. B907, 400 (2016).
 - [10] S. Bloch, M. Kerr, and P. Vanhove, Compos. Math. 151, 2329 (2015).
 - [11] S. Bloch, M. Kerr, and P. Vanhove, Adv. Theor. Math. Phys. 21, 1373 (2017).
 - [12] S. Borowka, J. Carter, and G. Heinrich, J. Phys. Conf. Ser. 368, 012051 (2012).
 - [13] S. Borowka, J. Carter, and G. Heinrich, Comput. Phys. Commun. 184, 396 (2013).
 - [14] W. Hollik, U. Meier, and S. Uccirati, Nucl. Phys. B731, 213 (2005).
 - [15] A. Freitas, W. Hollik, W. Walter, and G. Weiglein, Nucl. Phys. B632, 189 (2002).
 - [16] A. Alekseyevs, S. Barkanova, Y. Bystritskiy, A. Ilyichev, E. Kuraev, V. Zykunov, Eur. Phys. J. C72 2249 (2012).

- [17] A. Aleksejevs, S. Barkanova, V. Zykunov, E. Kuraev, Phys. Atom. Nucl. 76 888-900 (2013).
- [18] A. Aleksejevs, S. Barkanova, Y. Bystritskiy, E. Kuraev, V. Zykunov, Phys. Part. Nucl. Lett. 12 no.5, 645-656 (2015).
- [19] A. Aleksejevs, S. Barkanova, Y. Bystritskiy, E. Kuraev, V. Zykunov, Phys. Part. Nucl. Lett. 13 no.3, 310-317 (2016).
- [20] A. Aleksejevs, Phys. Rev. D. 98, 036021 (2018).